ALEPH 94-095
PHYSIC 94-082
T. Medcalf and I. Quazi
17.06.1994

Search for the decay $Z \rightarrow S\gamma$, where S is a scalar

T. Medcalf and I. Quazi
Royal Holloway

June 16, 1994

1 Introduction

In models in which the Z is composite, it is natural to expect it to decay to the scalar combination of the same preonic constituents (S), plus a photon, provided that $m_S < m_Z$. Although similar to the Higgs, S will have couplings different from those predicted for the Higgs by the Standard Model or by its extensions, but certain features of scalar couplings can be used as a guide to search for its decays, and couplings of the scalar to light fermions should be depressed due to chirality constraints. However radiative Z-decay events which would otherwise have a low branching ratio, such as $Z \rightarrow \ell^+\ell^-\gamma, gg\gamma, q\bar{q}\gamma$ or $\gamma\gamma\gamma$ could be enhanced. From [1] the width of $Z \rightarrow S\gamma$, for S having colourless constituents, is :

$$\Gamma(Z \rightarrow S\gamma) = \frac{\alpha}{96\Lambda_{eff}^2} \cdot \frac{(M_Z^2 - m_S^2)^3}{M_Z^3} \quad (1)$$

where Λ_{eff} is an effective subconstituent mass. Taking the value of Λ to be close to 1 TeV, the width becomes of the order of a few MeV. The detector resolution after fitting (section 5), is significantly worse than this being close to 0.1 GeV/c^2 when S decays to two electrons or to two muons and 2.5 GeV/c^2 when S decays to two taus. If the preonic constituents of S are coloured [2], then a larger width could be expected ($\alpha \rightarrow 3\sqrt{2}\alpha_s Q^2$, where Q is the preonic charge).

The processes $e^+e^- \rightarrow Z \rightarrow S\gamma \rightarrow \ell^+\ell^-\gamma$ or $gg\gamma$ or $q\bar{q}\gamma$ are searched for and 95% C.L. branching ratios limits set against these decays using 1990, 1991 and 1992 data and cuts similar to the excited lepton and quark searches.

Limits published previously [3] are 1.1×10^{-4} for e^+e^- and $\tau^+\tau^-$, 9×10^{-5} for $\mu^+\mu^-$ channels, and 4.7×10^{-4} for hadrons, up to 89 GeV (86 GeV only in the hadronic channel), and the searches start at 30 GeV (L3) or 60 GeV (OPAL). Additionally resonances in e^+e^- collisions have been searched for up to 47.8 GeV [4].

2 Analysis Event Samples

For each search, data, background and signal event samples were selected as follows: the data sample used all good events from 1990, 1991 and 1992 corresponding to approximately 41pb^{-1}, that is, 1,112,000 hadronic events.

For the leptonic channels the background was generated to be equivalent to approximately 10 times the amount of real data i.e. 410pb^{-1}, using physics generators modified

to pass on to the detector simulation only events which passed loose kinematical cuts. The generators used were, for $e^+e^- \to e^+e^-\gamma$ the first order QED generator BHABAMC [5, 6], and for $\mu^+\mu^-\gamma$ and $\tau^+\tau^-\gamma$, KORALZ [7]. This latter generator contains some higher order corrections and is expected to describe QED fairly well, although second order final state radiation is missing. For $\gamma\gamma$ (no events selected) and $q\bar{q}$ background to the leptonic channels (small) approximately 1.1 times and 2.5 times the amount of real data were used respectively, at the peak centre of mass energy. For the hadronic channels, the standard Aleph production for Monte Carlo $q\bar{q}$ events (based on Jetset 7.3 [8]) was used, with a statistic of approximately 2 times data.

To see how effective the cuts were and to calculate the detection efficiencies for each channel a signal Monte Carlo was used. In every case it was the Higgs generator [9], set for Higgs+photon production, and decay of the Higgs to the appropriate exclusive channel. Some modification was required to generate the hadronic channel with significant S-width: sets of simulated events with negligible width and with width equal to .05S-mass were both generated. 1000 events in the leptonic channels (2000 events in the hadronic channels) of the signal Monte Carlo at each mass in 5 GeV/c^2 step intervals (starting at a mass of 5 GeV/c^2, plus 86,87,88 and 89 GeV/c^2) were generated. For 10,45 and 85 GeV and higher in the hadronic channels only the simulated events were passed through the 1990, 1991 and 1992 detector simulations, in the appropriate proportions. At the other masses fast generator-level fiducial cuts were used and these results scaled against the full simulations, by interpolation: scaling factors were ~ 0.9. In the leptonic channels full detector simulation was used for all masses. These efficiencies, shown in figures 1 and 2, are used to set the 95% confidence level limits on the branching ratio products (BR($Z \to S\gamma$) $\times$ $BR(S \to \ell^+\ell^-$ or gg or $q\bar{q}$)) In general, the efficiencies are of the order of 60 % and above, in the leptonic channels, and rather lower in the hadronic channels.

3 Data Selection

3.1 Run and event selection

The event selection was made for all runs which satisfied the 'standard searches' run selection. Those 1992 runs with a TPC problem were only used if the fault had been corrected. For those runs for which the luminosity was unavailable, the Monte Carlo was normalized to the number of hadronic events.

3.2 Charged particle track definition

Energy flow charged particle tracks were required to have a momentum of at least 0.5 GeV/c, be reconstructed with at least four space coordinates in the TPC and originate from a cylinder of length 140 mm and radius 25 mm coaxial with the beam axis and centred at the interaction point. Furthermore, to be counted as 'good tracks', they must form an angle with the beam direction of at least 18.2°. In the leptonic channels only events with one, two or four charged tracks are accepted for further analyses. For events with two and four charged tracks, the total charge must be zero. In the hadronic channels, only events with thrust ≤ 0.95 were considered: these were forced (by varying Ycut) into a 3-jet configuration using the JADE clustering algorithm [10]. Thrust distri-

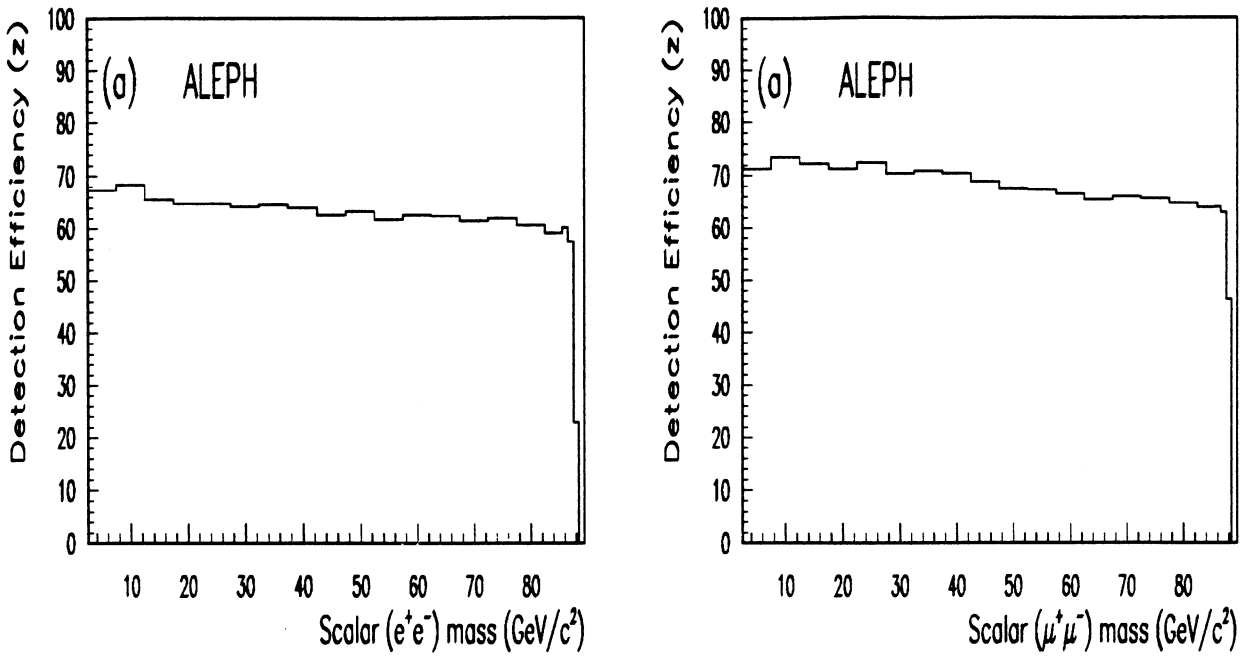

Figure 1: The efficiency of fully simulated signal Monte Carlo selection for a) $S(e^+e^-)\gamma$ production b) $S(\mu^+\mu^-)\gamma$ production.

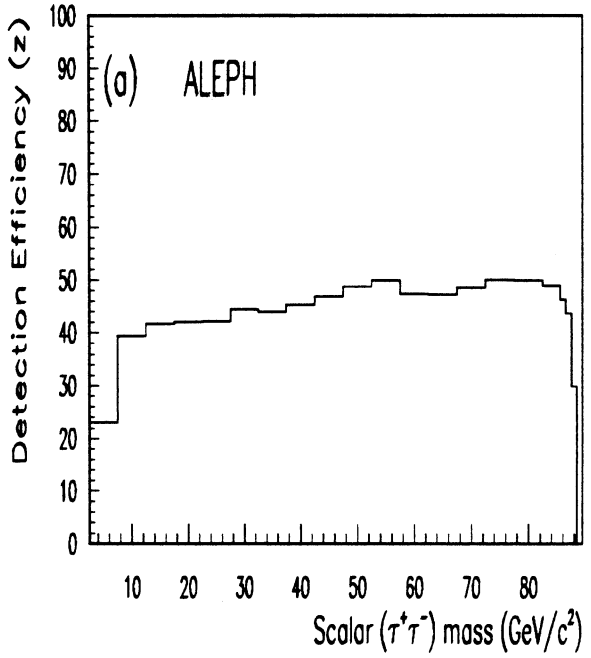

Figure 2: The efficiency of fully simulated signal Monte Carlo for the $S(\tau^+\tau^-)\gamma$ channel.

butions are shown in figure 3. Events were also retained if only two jets could be made. It was then required that the 'good track' multiplicity of two of the jets should be each at least 4 (except where there was only one non-photonic jet, when 7 charged tracks were required) and that at least 90% of the energy of the other jet should belong to a single photon (same definition as for the leptonic channels, see below).

3.3 Calorimetric cluster and photon definition

Initially, a search for at least one hard photon was performed using ECAL energies corrected for overlap, crack, leakage and saturation effects. To be validated as a photon, an ECAL cluster has to be identified as an electromagnetic object by both Gampec and Energy Flow. Finally to be considered in the analysis, the photon must have an energy greater than 3 GeV and its flight path must form an angle with the beam direction of at least 18.2°.

4 Event Selection for Scalar candidates

4.1 Kinematical Selection

The photon energy spectrum in radiative leptonic Z decays falls rapidly with increasing energy (e.g. unbroken line in figure 4.a). The photon spectrum for S production is dependent on two kinematical variables: the centre of mass collision energy and the scalar particle mass. At fixed centre of mass energy and scalar mass, the photon spectrum is a delta-function (figure 4.a), where the energy of the photon is determined from the kinematics (equation 1). As the mass of the scalar increases, the kinematics force the photon energy to decrease (figure 4.b) so that near the Z boson mass, the photon energy is so small that the signal becomes completely indistinguishable from the electroweak background (figure 4.a). The objective then is to remove most of the radiative background whilst at the same time to achieve a good efficiency up to as high a scalar mass as possible. A photon energy cut of 3 GeV has been used, and cannot be reduced further because of background. This results in zero efficiency for a scalar mass of approximately 89 GeV/c^2 and above.

In general, events containing final state photons in the background have a low energy photon close to a track or a charged jet. (e.g. figure 4.c). For the scalar signal at low mass, the S particle moves very fast and thus the charged tracks from the S decay are relativistically collimated. Thus $\theta_{\gamma,trk}$ is large (figure 4.c). As the mass increases, the relativistic boost decreases so that the charged tracks become less collimated and in the limit of high mass, the decay becomes isotropic. Thus, each selected photon is required to be at least 30° away from each charged track. Where more than one photon satisfies all the criteria, the most energetic is retained for the subsequent analysis. If multiple-photon events are discarded, the data and background fail to agree, because of the incompleteness of the Monte Carlos.

The majority of leptonic background consists of two-track e^+e^-, $\mu^+\mu^-$ and $\tau^+\tau^-$ events with the charged tracks back-to-back (e.g. unbroken line in figure 4.d), i.e. the angle between the tracks is 180°. Photon emission mainly occurs at low energy so that the photon is usually very close to the track and the two charged tracks in the event

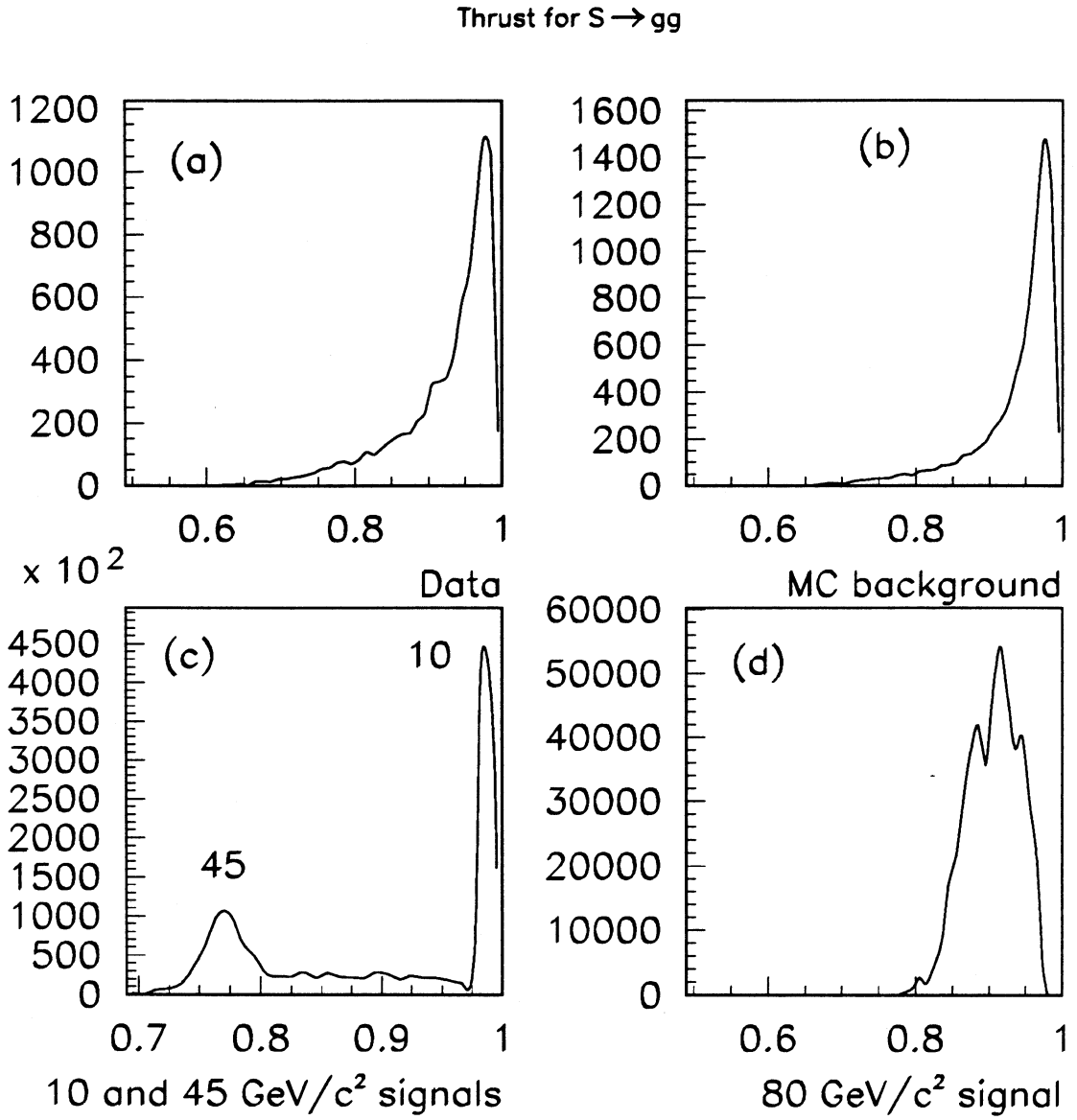

Figure 3: Thrust distributions (a) data, (b) background Monte Carlo, (c) 45 GeV scalar mass signal and (d) 80 GeV signal.

are *almost* back-to-back, i.e. the angle between the tracks depends on the energy of the photon (from momentum and energy conservation). Hence only those events are selected where the two charged track acollinearity is smaller than 178° but greater than 10° (figure 4.d). The latter part of the cut is used to remove photon conversions since in general the tracks arising from a conversion are very close together. The acollinearity cut is not applied to the four track topology. The objective of these cuts is to remove as much electroweak radiative background as possible. The thrust cut in the hadronic events, which have the same kinematics, has essentially the same effect.

4.2 Search for $e^+e^- \to S\gamma \to e^+e^-\gamma$

The total ECAL energy measured on the wire planes minus the photon energy (as given by the cluster localized on the cathode pads) was required to be larger than 75% of the total available energy once the photon has been radiated,

$$El_{\rm nor} = \frac{E_{wires} - E_\gamma}{E_{\rm cms} - E_\gamma} > 0.75$$

This requirement alone isolates, with a high efficiency, final states where electromagnetic energy dominates. Finally, in order to check the electron identification, at least one charged track must be positively identified by QEIDO.

The final sample consists of 1530 $e^+e^-\gamma$ events compared to 1836.3 predicted from the hard radiative electroweak process $e^+e^- \to e^+e^-\gamma$ as seen in table 1. The disagreement is understood as being due to the limitations of Bhabamc generator. Because only one photon is generated, its spectrum is much harder than is that of the hardest photon produced by a higher order generator: comparing with KoralZ, this effect is expected to be $\sim$ 15%, which brings these numbers into statistical agreement.

		Monte Carlo			
Analysis stage	DATA	$e^+e^-\gamma$	$\mu^+\mu^-\gamma$	$\tau^+\tau^-\gamma$	$q\bar{q}$
Selected events with $E_\gamma > 3$ GeV	15297	2402.7	1967.7	1722.9.3	674.6
After isolation (30°) cut	5005	2033.9	1226.0	746.0	283.0
After acollinearity	3993	2008.9	1101.8	670.3	36.7
After $El_{\rm nor} > 0.75$ cut	1541	1838.6	0.0	3.0	0.0
After QEIDO	1530	1836.3	0.0	2.0	0.0

Table 1: Breakdown of events through the $e^+e^- \longrightarrow e^+e^-\gamma$ analysis for the scalar search. A match between data and Monte Carlo should be expected after the acollinearity cut since the Monte Carlo has been generated with prior (loose) kinematical cuts.

4.3 Search for $e^+e^- \to S\gamma \to \mu^+\mu^-\gamma$.

Initially, only those events were selected where the total visible electromagnetic energy, except that corresponding to the photon, is small. For this, the total ECAL energy

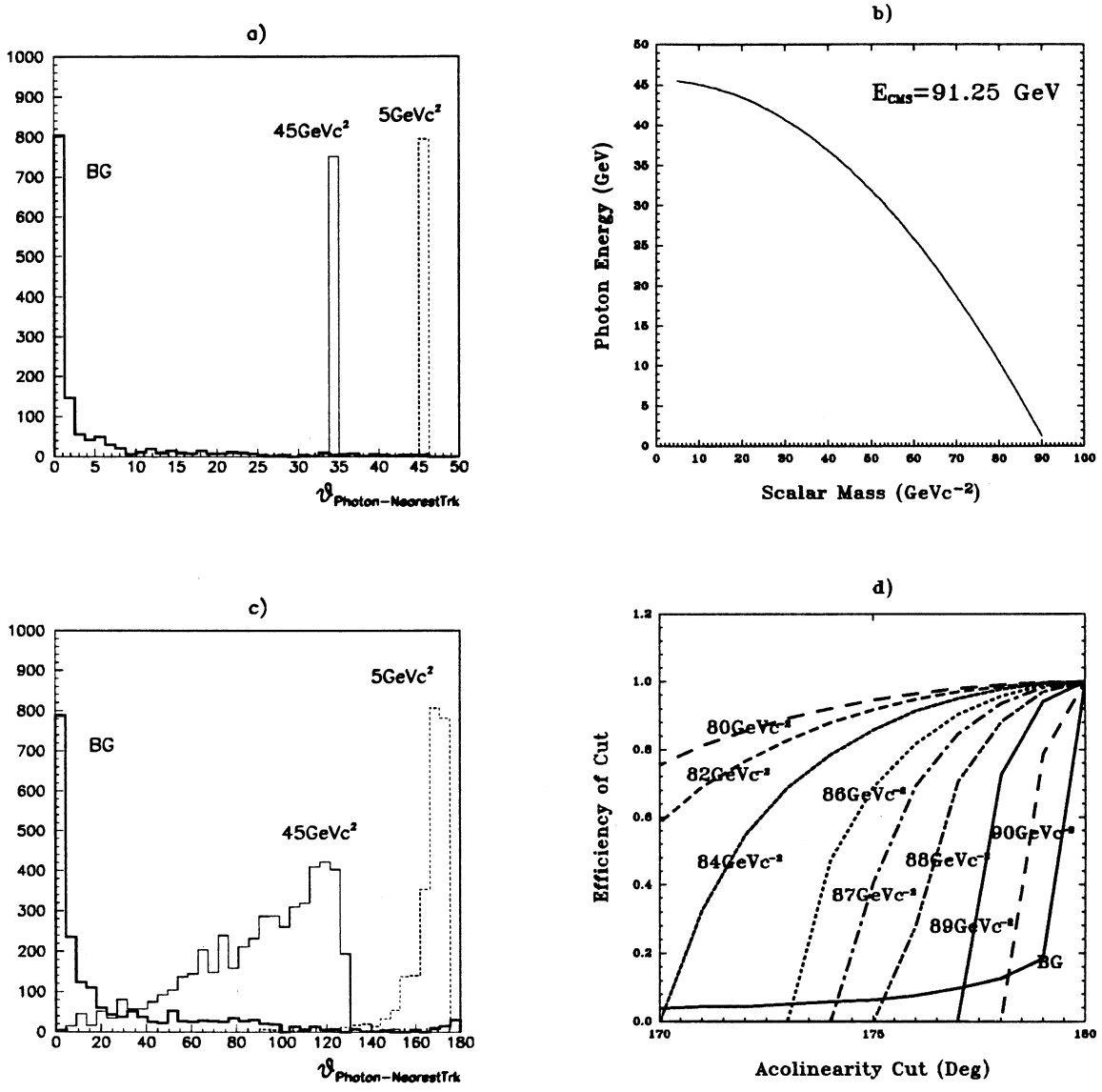

Figure 4: Kinematics of scalar boson production. a) Photon energy spectrum for the background (solid line) and 5 and 45 GeV/c^2 scalar masses (broken lines). b) The variation of photon energy with scalar mass determined at the peak CMS energy. c) The angle between the photon and the nearest charged track for the background (solid line) and 5 and 45 GeV/c^2 masses (broken lines). d) The efficiency of the charged track acollinearity cut as a function of the acollinearity angle

measured on the wire planes minus the photon energy was required to be smaller than 10% of the total centre-of-mass energy,

$$E2_{\rm nor} = \frac{E_{wires} - E_\gamma}{E_{cms}} < 0.1$$

This removes all the bhabha events and a large fraction of the $\tau^+\tau^-$ events. A second cut removes all remaining background, selecting those events where the sum of the charged particle momenta and of the photon energy is larger than 80% of the total centre-of-mass energy,

$$E3_{\rm nor} = \frac{\sum_{tracks} P + E_\gamma}{E_{cms}} > 0.8$$

In order to check the muon identification, at least one charged track must be positively identified by QMUIDO.

The final sample consists of 1128 $\mu^+\mu^-\gamma$ events compared to 1154.2 predicted from the hard radiative electroweak process $e^+e^- \to \mu^+\mu^-\gamma$ as seen in table 2.

		Monte Carlo			
Analysis stage	DATA	$\mu^+\mu^-\gamma$	$e^+e^-\gamma$	$\tau^+\tau^-\gamma$	$q\bar{q}$
Selected events with $E_\gamma > 3$ GeV	15297	1765.7	4154.9	1749.2	674.6
After isolation (30°) cut	5005	1342.7	2212.1	757.7	283.0
After acollinearity	3993	1178.0	2031.4	680.9	36.7
After $E2_{\rm nor} < 0.1$ cut	1528	1172.0	5.8	184.2	5.0
After $E3_{\rm nor} > 0.80$ cut	1130	1162.0	4.4	7.3	0.0
After QMUIDO	1128	1154.2	0.0	7.3	0.0

Table 2: Breakdown of events through the $e^+e^- \longrightarrow \mu^+\mu^-\gamma$ analysis for the scalar search. A match between data and Monte Carlo should be expected after the acollinearity cut.

4.4 Search for $e^+e^- \to S\gamma \to \tau^+\tau^-\gamma$.

For this study, events with two or four good tracks are considered, and they must have failed the e^+e^--channel cut on the ECAL wire-energy. Calculation of the missing mass is used to distinguish tau-events from events without neutrinos (lower) and events without a Z (higher): it is defined from the charged tracks alone, ie

$$E^2_{miss} = (E_{emcs} - \sum_{tracks} E_{track})^2 - (\sum_{tracks} \underline{p})^2$$

The two track topology is considered first. To remove events belonging to the processes $e^+e^- \to e^+e^-\gamma$ and $e^+e^- \to \mu^+\mu^-\gamma$, the missing mass square is required to be larger than 500 GeV/c^2. It is also required to be less than 6500 GeV/c^2, as such events are very rare in the signals but occur occasionally in the data, from channels not simulated in the background Monte Carlo. Finally two more cuts were applied on all events in this topology to remove remaining backgrounds. First, the sum of the charged particle

momenta and of the associated ECAL cluster energies, normalized to the available centre-of-mass energy after subtraction of the photon energy,E_{chsum}, was required to be less than 1.1. This cut removes the tail of $e^+e^- \to e^+e^-\gamma$ events where, for example, another hard photon is emitted along the track direction. Secondly, the sum of the charged particle momenta was required to be less than than 80% of the total available energy (after subtraction of the radiated photon energy, variable p_{sum}. This cut mainly removes the remnant contribution from $e^+e^- \to \mu^+\mu^-\gamma$. At this stage there are 603 data events.

Next four charged track candidates are considered. To remove background from events where the main part of the final state escapes detection in the beam directions, the missing mass squared is required to be smaller than 6000 ($GeV/c^2)^2$. $ee\gamma\gamma$ events of the type where one photon converts to an e^+e^- pair are rejected by requiring the missing mass to be greater than 250 ($GeV/c^2)^2$. Tau candidates decaying into three charged particles are selected as triplets of tracks with a total electric charge ± 1 and an invariant mass smaller than 1.6 GeV/c^2 (the pion mass being assumed for the charged particles). If more than one triplet fulfills these conditions, the events is discarded (no such events occur in signal Monte Carlo).

The final sample consists of 886 $\tau^+\tau^-\gamma$ events compared to 840.3 predicted from the hard radiative electroweak process, $e^+e^- \to \tau^+\tau^-\gamma$ plus 25.9 other background events, as seen in table 3,

		Monte Carlo			
Analysis stage	DATA	$\tau^+\tau^-\gamma$	$e^+e^-\gamma$	$\mu^+\mu^-\gamma$	$q\bar{q}\gamma$
Selected events with $E_\gamma > 3$ GeV	15297	1749.2	2402.7	1457.1	165.0
After isolation (30°) cut	5005	681.0	2034.0	1290.7	156.0
After acollinearity (2 trks only)	3993	662.6	2009.0	1248.5	55.0
After missing mass (2 trks only)	2301	652.5	133.1	9.5	15.1
After E_{chsum} (2 tracks only)	696	617.4	8.5	9.5	10.6
After p_{sum} (2 tracks only)	603	580.6	6.5	3.8	1.3
After isolation (30°) (4 trks only)	829	285.8	24.2	1.3	105.6
After missing mass	726	264.7	6.5	1.1	83.0
After inv. mass (1.6 GeV/c^2)	283	259.7	6.1	0.0	8.2
Final sample	886	840.3	12.6	3.8	9.5

Table 3: Breakdown of events through the $e^+e^- \longrightarrow \tau^+\tau^-\gamma$ analysis for the scalar search. A match between data and Monte Carlo should be expected after the acollinearity cut (photon isolation cut in the 4-track case).

4.5 Search for $e^+e^- \to S\gamma \to q\bar{q}\gamma$ or $gg\gamma$.

At very high mass (80 GeV scalar and above, where the jets are back-to-back and the photon soft) too many signal events are lost by the photon isolation cut (no charged tracks above .5 GeV/c), if it is maintained at 30°, so it reduced to 15°, in the searches specific to these masses. Efficiencies and final photon samples are shown in figure 5, where the signal Monte Carlo events are from the gluonic decay with negligible intrinsic

width, but the $q\bar{q}$ decay is very similar, and the inclusion of significant width makes a measurable difference at high mass only.

The number of data-events accepted is 1176 (including 301 allowed only by the relaxed cuts for the high mass ranges), compared with 1688 (355 from the relaxed cut) from the background Monte Carlo, at a statistic of 1.91, leaving a $\sim$ 20% underestimate due to the simulation.

Each S-mass that was simulated was searched for by requiring a monochromatic photon of energy (within $\pm 2\sigma$ of the photon energy resolution),

$$E_\gamma = 0.5\frac{m_Z^2 - m_S^2}{m_Z}$$

where around 100 data-events lie in each range.

5 Invariant mass reconstruction

In general the invariant mass of a system of n particles is trivially calculated from the well known relation :

$$XM^2 = \left(\sum_{i=1}^{n} E_i\right)^2 - \left(\sum_{i=1}^{n} p_{x_i}\right)^2 - \left(\sum_{i=1}^{n} p_{y_i}\right)^2 - \left(\sum_{i=1}^{n} p_{z_i}\right)^2 \qquad (2)$$

Because of the intrinsic error in the momentum and energy measurement due to the detector, the invariant mass resolution for an $e\gamma$ or $\mu\gamma$ pair as calculated from equation 2 is rather poor and is of the order of about 2 GeV/c^2 full width half maximum (FWHM).

However the mass resolution can be improved by using the angular measurements and rescaling the energies of the charged particles and the photon. Using these re-scaled values, the invariant mass resolutions are about 0.5 GeV/c^2 FWHM for the $e^+e^-\gamma$ and $\mu^+\mu^-\gamma$ channels. In the high mass region above 45 GeV/c^2, all these resolutions are found to be approximately independent of the mass of the particles. For example, $\mu^+\mu^-$ efficiencies are shown in figure 6.

Reconstructing the invariant mass for the $\tau^+\tau^-\gamma$ channel is slightly more complicated although the general principle is the same. The basic concept is that τs produced at the Z peak are so energetic that all their decay products are relativistically collimated to the extent that the direction of the charged track detected may be taken, with little error, to be the direction of the τ. After re-scaling the momenta of the charged tracks and the energy of the photon, the excited lepton resolution is found to be of the order 5.0 GeV/c^2 FWHM.

In the hadronic channel essentially the same process is followed. The jets are projected onto the event plane (defined by the thrust- and major-axes) and then treated in exactly the same way as the particles above.

6 Limits for Scalar Production

In the leptonic channels the branching ratio limit is set by a bin by bin calculation based on the Poison distribution. The number of events predicted comes from the efficiency, assuming a branching ratio of 1.

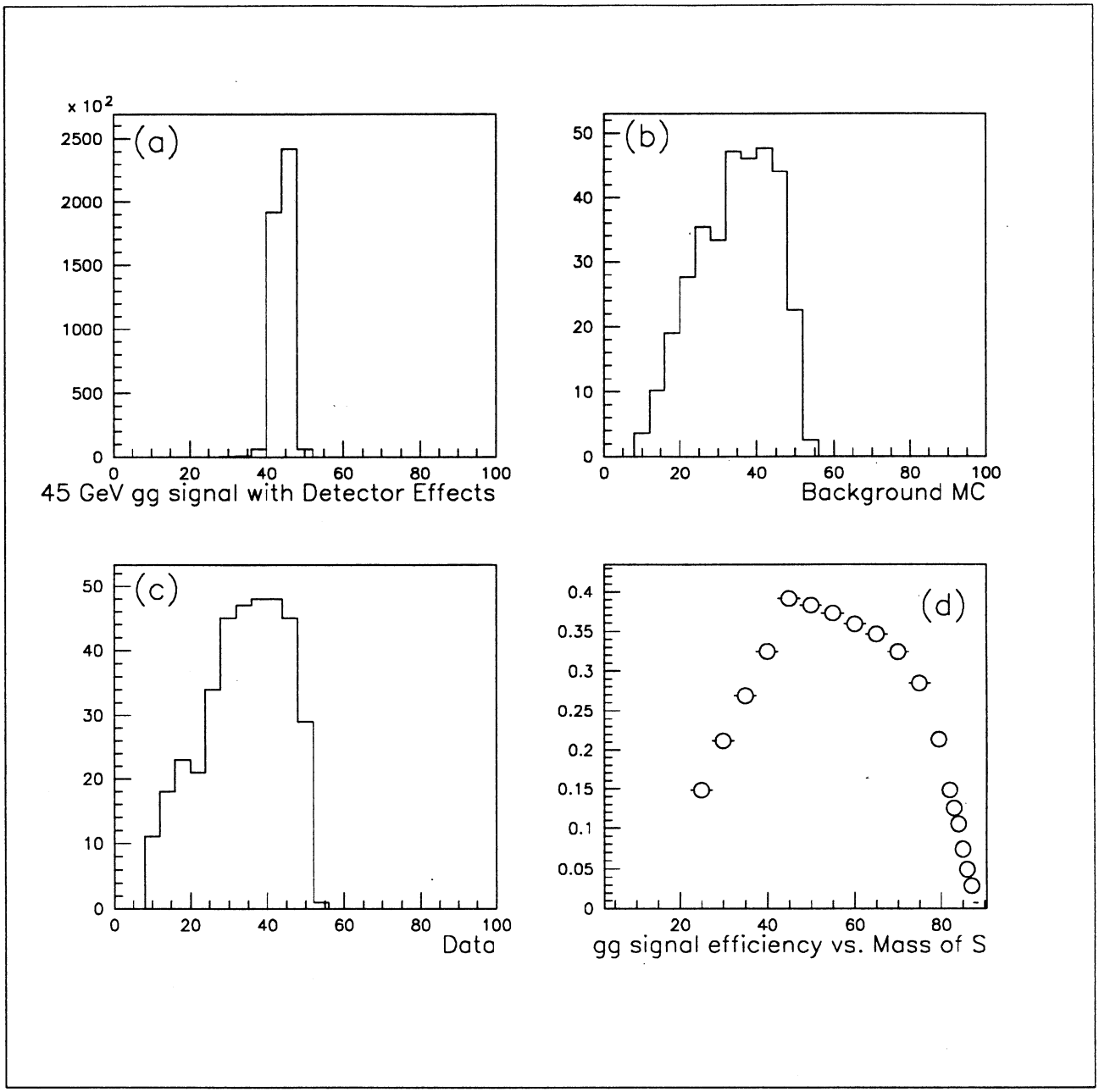

Figure 5: Final photon samples for (a) signal: 45 GeV scalar mass, (b) background Monte Carlo, (c) data and (d) efficiency of fully simulated signal Monte Carlo as a function of scalar mass for $S \rightarrow gg$.

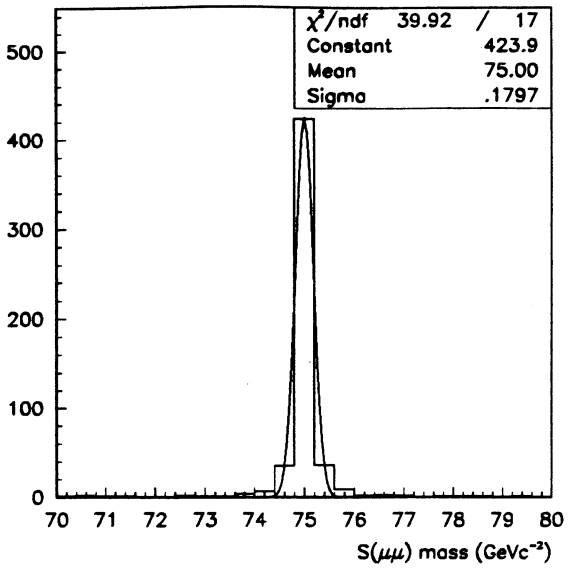

Figure 6: The resolution for the $S(\mu^+\mu^-)\gamma$ channel for a scalar of mass 75 GeV/c^2.

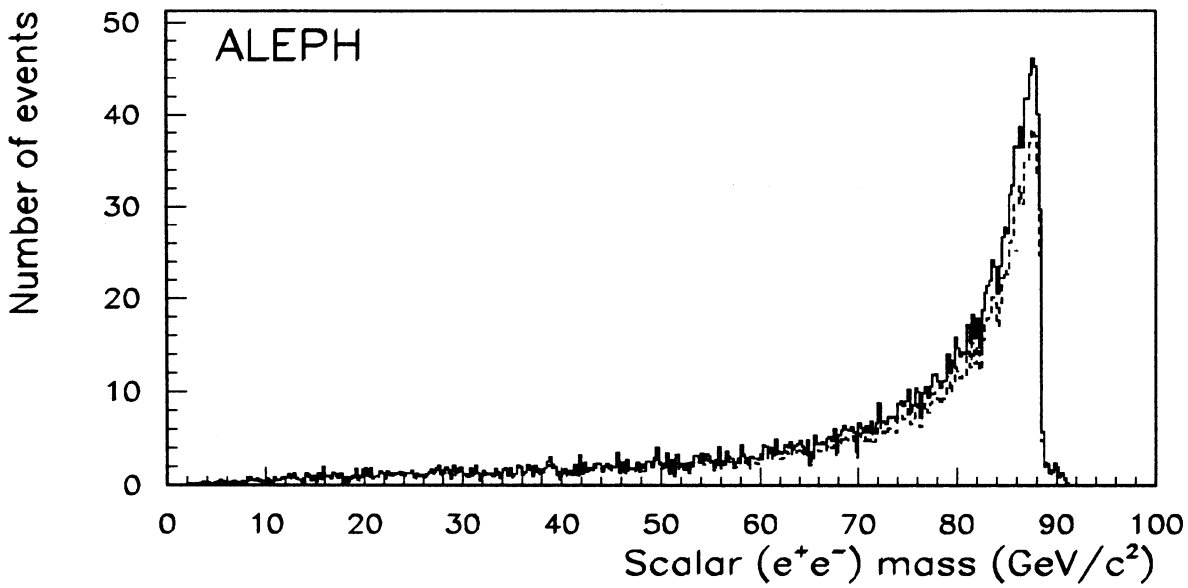

Figure 7: The e^+e^- invariant mass: rescaled simulation.

The final invariant mass and branching ratios plots are given in figures 8, 9 and 10 for the processes $Z \to S(e^+e^-)\gamma$, $Z \to S(\mu^+\mu^-)\gamma$ and $Z \to S(\tau^+\tau^-)\gamma$ respectively. Using the arguments advanced when discussing table 1, $e^+e^-\gamma$ background Monte Carlo for the $Z \to S(e^+e^-)$ channel has been reweighted before the branching ratio limit was calculated. The uncorrected plots are shown in figure 7.

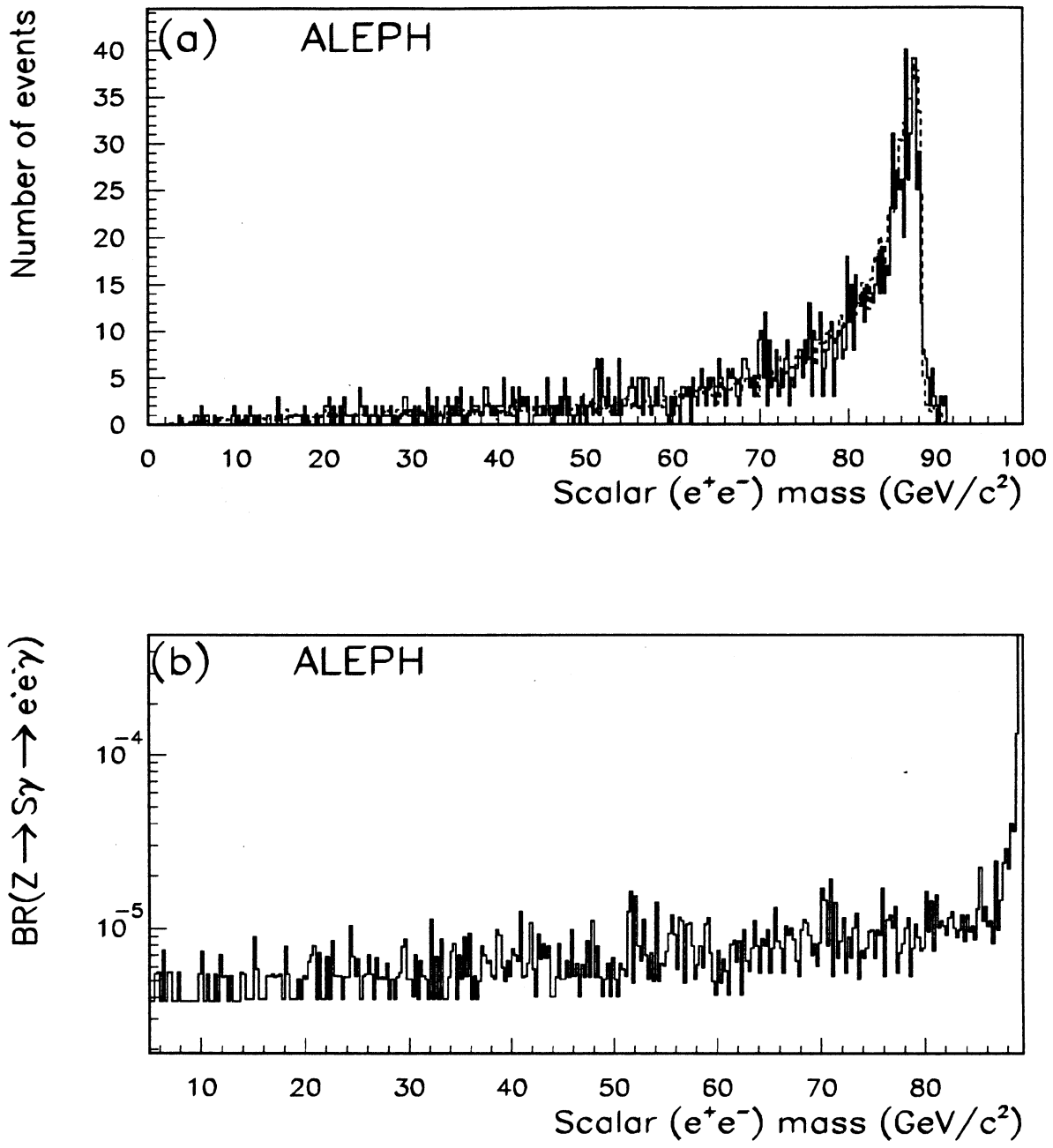

Figure 8: Reweighted plots for a) The e^+e^- invariant mass. The background has been smoothed for presentational purposes. (b) The 95% C.L. branching ratio of $Z \to S(e^+e^-)\gamma$. Reweighting the background Monte Carlo has no noticeable effect on the coupling curve.

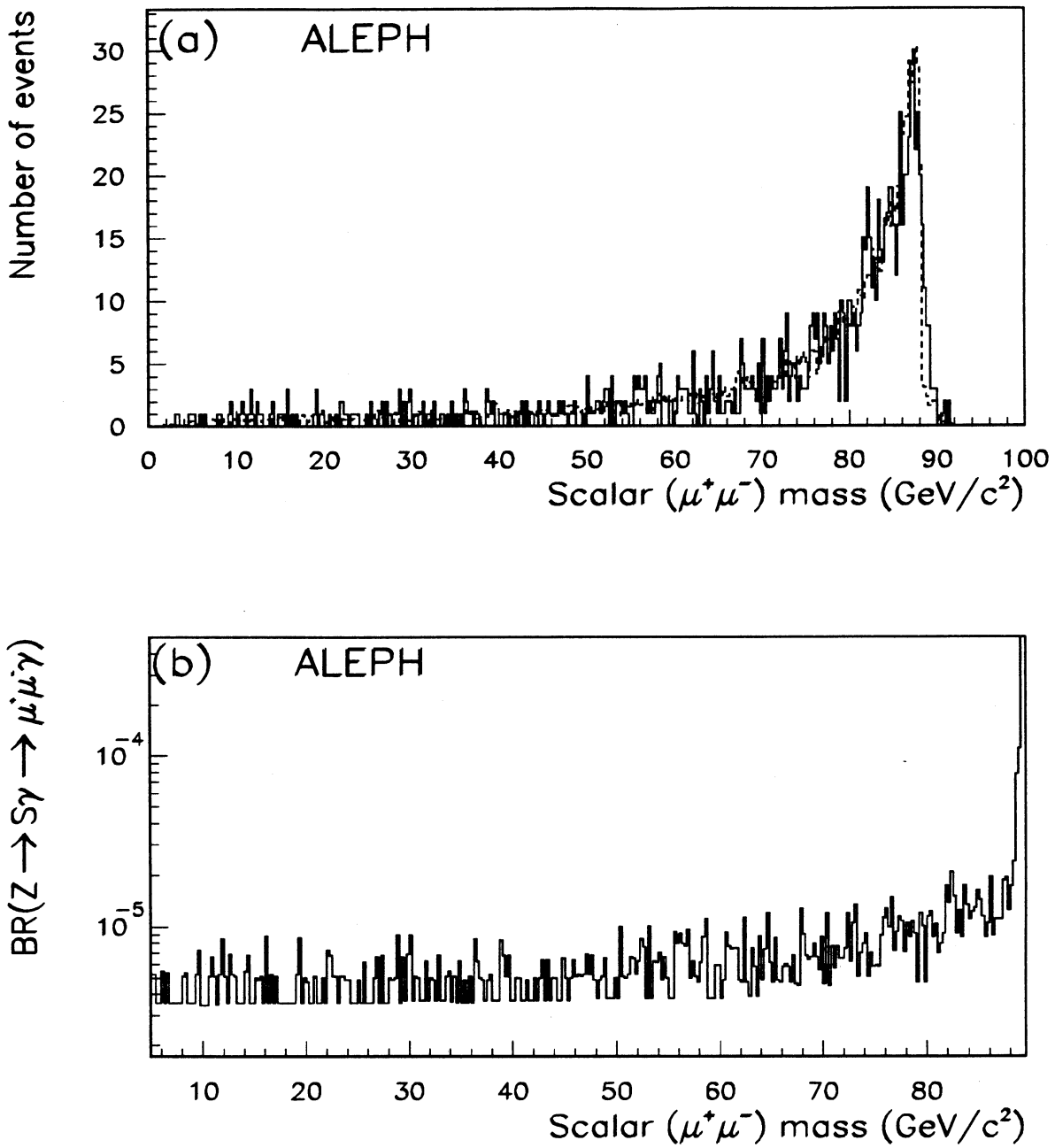

Figure 9: a) The $\mu^+\mu^-$ invariant mass. The background has been smoothed for presentation purposes. b) The 95% C.L. branching ratio of $Z \to S(\mu^+\mu^-)\gamma$.

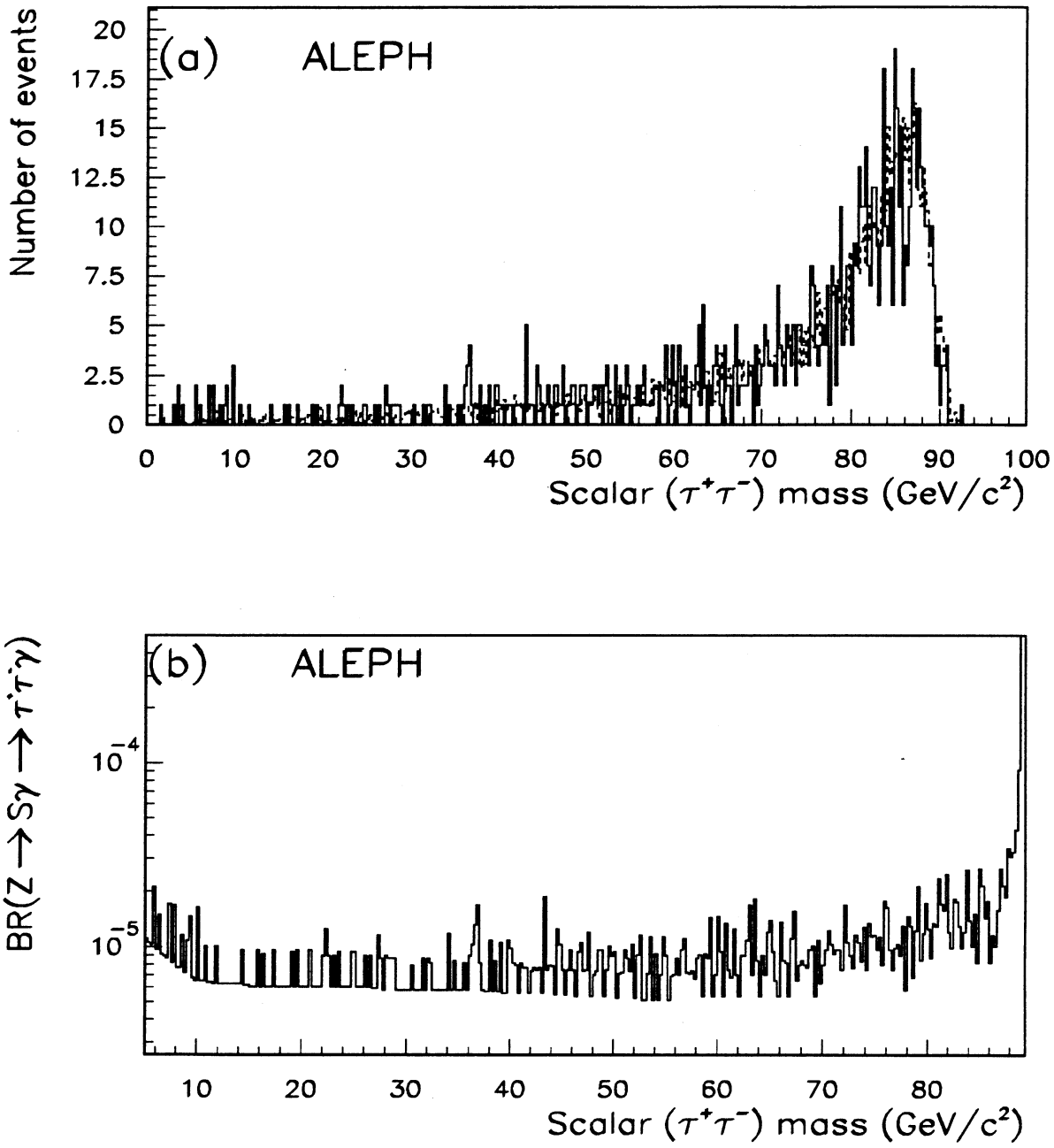

Figure 10: a) The $\tau^+\tau^-$ invariant mass. The background has been smoothed for presentation purposes. b) The 95% C.L. branching ratio $Z \rightarrow S(\tau^+\tau^-)\gamma$.

In the hadronic channel plots were made both of the jet-jet invariant mass of the rescaled events and of E_γ versus the jet-jet invariant mass. These plots were then fitted with MINUIT, using

$$\chi^2 = \sum_i [D_i - f_1 B_i - f_2 S_i]^2 / \sigma_i^2$$

where D_i, B_i, S_i are the event-numbers in bin i in the data, background Monte Carlo and signal Monte Carlo respectively, and σ_i^2 is the variance. The approximation $\sigma_i^2 = D_i$ was used, justified by rebinning so that $D_i \geq 6$. The χ^2 per degree of freedom for the MINUIT fits was close to unity. f_1 and f_2 are the best-fit factors for the background Monte Carlo and for the signal and f_1 was typically around 1.17, the usual discrepancy between JETSET 7.3 and data. 95% confidence level limits to the branching ratio,

$$BR \leq f_2 + 1.64\sigma_2,$$

consistent with the Beyesian concept. Limits are shown in figure 11 (gluon-decay) and figure 12 (quark-decay).

7 Conclusions

Using a data sample corresponding to approximately 1,112,000 hadronic Z decays, the process $e^+e^- \to \ell^+\ell^-\gamma$, (where ℓ = e, μ or τ)has been studied in order to search for deviations from Standard Model predictions. No such evidence has been found in the searches for $S(l\bar{l})$ (where $l = e$, μ or τ).

No evidence has been found of a scalar boson and branching ratios are set at $< 4\times10^{-6}$ at 95% confidence level, for each of the leptonic decays and $< 5 \times 10^{-5}$, when the decay is hadronic (quarks or gluons). These branching ratios very much improve previous limits [3] by approximately 2 orders of magnitude in the leptonic channels, and 1 order of magnitude in the hadronic channels.

It can be concluded therefore that the measured distributions as well as the rates of the processes $e^+e^- \to \mu^+\mu^-\gamma$ and $e^+e^- \to \tau^+\tau^-\gamma$, observed in conditions similar to those of a hard radiative process, are in good agreement with Standard Model predictions. For the process $e^+e^- \to e^+e^-\gamma$, there is not very good agreement between the data and the Monte Carlo but the disagreement is understood and is associated to lack of higher orders in the Monte Carlo. In the hadronic channels, it is well known that Jetset 7.3 does not simulate the photon-rate very well, but there no evidence for a mass resonance decaying to $q\bar{q}$ or gg below the Z-mass, in the range 20-88 GeV.

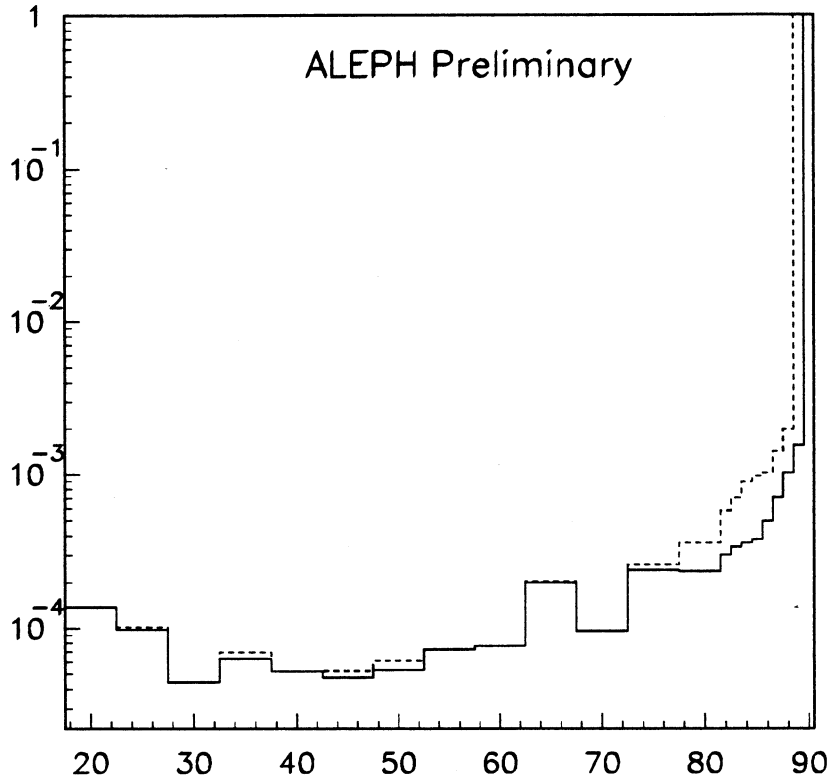

Figure 11: Limits on branching ratio $Z \rightarrow S(gg)\gamma$. Continuous line: width less than experimental resolution. Dotted line: width of 0.05 $\times$S-mass.

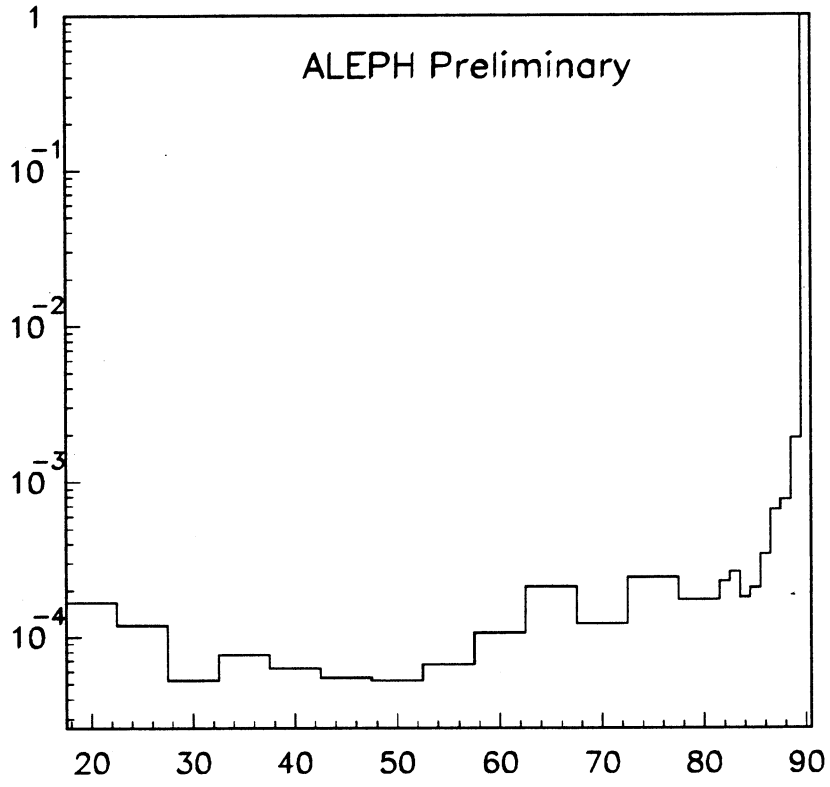

Figure 12: Limits on branching ratio $Z \to S(q\bar{q})\gamma$.

References

[1] G. Altarelli *et al.* (eds.), "Z Physics at LEP1", CERN 89-08, vol. 2, 204-205

[2] F. M. Renard, Phy. Lett. **126B** (1983) 59.

[3] L3 Collab. B. Adeva *et al.*, Phys. Rev. Lett. **67** (1991) 2418. OPAL Collab. P. D. Acton *et al.*, Phys. Lett. **B273** (1991) 338.

[4] MARK-J Collab., B. Adeva *et al.*, Phys. Rev. Lett. 54 (1984) 1887.

[5] M. Bohm, A. Denner and W. Hollik, Nucl. Phys. **B304** (1988) 687.

[6] F. Berends, R. Kleiss and W. Hollik, Nucl. Phys. **B304** (1988) 712.

[7] S. Jadach, B. Ward and Z. Was, Comput. Phys. Comm. **66** (1991) 276.

[8] T. Sjostrand and M. Bengtson, Comput. Phys. Comm. **43** (1987) 367,

[9] A. Van Proeyen, Phys. Rev. **D20** (1979) 81, D. R .T. Jones,S . T. Petkov, Phys. Lett.84B (1979) 440, A. S. Schwarz, Aleph Note 88-198, P. Janot, Aleph Note 89-03

[10] JADE collab., W. Bartel *et al.*, Z. Phys. C 33 (1986) 23.
JADE collab., S. Bethe *et al.*, Phys. Lett. B 213 (1988) 235.